Shift of peaks and dips in elastic scattering in the Chou-Yang model

D. J. Clarke and S. Y. Lo
School of Physics, University of Melbourne, Parkville, Victoria, Australia 3052

(Received 25 February 1974)

The effect of the logarithmic increase of total cross section of the pp interaction on the Chou-Yang model is investigated. It is found that (i) the positions of dips and peaks move inward towards smaller $|t|$ values as the energy increases and (ii) the height of the peaks increases logarithmically as a function of energy. Comparison with the model of Cheng and Wu is made.

I. INTRODUCTION

In recent pp elastic scattering in CERN ISR experiments the diffraction zero at $t \cong -1.4$ has been found.[1] This can be considered as strong evidence for the geometrical picture of high-energy scattering as advocated by Chou and Yang. On the other hand, one is confronted with the data on the pp total cross section,[2] which is increasing logarithmically with energy. We have a paradox with a naive geometric picture where the total cross section $\sigma_{\text{tot}} \sim 2\pi R^2$ measures the radius of the proton. One solution is to assume the radius of the proton is increasing with energy. This may well be true but it has the apparent "unattractive" feature of a proton, which has a constant and finite radius as measured from e-p scattering, becoming one with a variable radius when it interacts strongly with another proton. There is yet another solution to this paradox, not requiring that the proton change its shape. It retains the same shape as measured by the e-p scattering experiment. Here we assume that the interaction strength has a logarithmic energy dependence phenomenologically. The model of Cheng and Wu is closer to the first solution. We would like to explore in this paper the consequences of the second solution.[3]

To be specific, in Sec. II we shall adopt the Chou-Yang model[4] formulated in terms of current-current interaction pictures,[5] and calculate the total and differential cross sections. In Sec. III we shall examine the qualitative features of the Chou-Yang model at high energies. The interesting points raised include the following:

(1) The positions of the dips and the peaks move in to smaller $|t|$ values as energy increases.

(2) The height of the first peak increases like $(\ln s)^2$, the height of the second peak like $(\ln s)^4$, and the height of the nth peak like $(\ln s)^{2n}$.

In Sec. IV we discuss the differences between our calculations and the model of Cheng and Wu.[6] We find that there are significant differences, which can be resolved in future experiments.

II. CHOU-YANG MODEL

The Chou-Yang model contains a very specific assumption as to the form of the S matrix, as a function of the impact parameter $\vec{b}$, for nucleon-nucleon scattering, and in the current-current formulation of the model it is postulated that, in the infinite-momentum frame,

$$S(s,\vec{b}) = \exp\Big[-2\pi\mu_0(s)\int\int d^3\kappa\, d^3\kappa' j_4^{(0)}(\vec{\kappa},0) j_4^{(0)}(\vec{\kappa}',0)\,\delta^{(2)}(\vec{b}-\vec{\kappa}'+\vec{\kappa}) - 2\pi\mu_1(s)\int\int d^3\kappa\, d^3\kappa' j_4^{(3)}(\vec{\kappa},0) j_4^{(3)}(\vec{\kappa}',0)\,\delta^{(2)}(\vec{b}-\vec{\kappa}'+\vec{\kappa})\Big], \tag{1}$$

where $j_4^{(0)}$ and $j_4^{(3)}$ are the fourth components of the isoscalar and isovector currents of the proton. The first expression with the interaction strength $\mu_0(s)$ is the vacuum exchange term, and the second expression with the interaction strength $\mu_1(s)$ is the $I=1$ exchange term. The scattering amplitude $\alpha(s,\kappa^2)$ for elastic proton-proton scattering is defined by the relation

$$i(2\pi)^6\delta^{(2)}(\vec{k}'-\vec{k}+\vec{\kappa})\delta^{(2)}(\vec{p}'-\vec{p}-\vec{\kappa})\delta(k_3'-k_3)\delta(p_3'-p_3)\alpha(s,\kappa^2) = \left\langle p',k'\right|\int\frac{d^2\vec{b}}{2\pi}\exp(i\vec{\kappa}\cdot\vec{b})[S(s,\vec{b})-1]\left|p,k\right\rangle, \tag{2}$$

where p, k and p', k' are the incoming and outgoing four-momenta of the protons, and $\vec{\kappa}^2 = -t$ is the transverse momentum squared. The amplitude is next decomposed into a sum of two terms the vacuum exchange term $\alpha_0(s, \kappa^2)$ and $I = 1$ exchange term $\alpha_1(s, \kappa^2)$.

It should be emphasized that α_0 is far more reliable than α_1. All the new findings in this paper come from the study of the behavior of α_0, and are quite insensitive to the particular form α_1 takes.

In performing numerical calculations, multiple-scattering terms of up to seventh order in $\alpha_0(s,\kappa^2)$ and first order in the smaller amplitude $\alpha_1(s, \kappa^2)$ are included thus:

$$-i\alpha_0(s,\kappa^2) = \mu_0(s)\langle\vec{\kappa}|j_4^{(0)}(0)|0\rangle\langle -\vec{\kappa}|j^{(0)}(0)|0\rangle - \frac{\mu_0^2}{2!}(s)\int\frac{d^2\kappa'}{2\pi}\sum_{\text{spin}}\langle\vec{\kappa}|j_4^{(0)}(0)|\vec{\kappa}'\rangle\langle\vec{\kappa}'|j_4^{(0)}|0\rangle\langle -\vec{\kappa}|j_4^{(0)}(0)|-\vec{\kappa}'\rangle\langle -\vec{\kappa}'|j_4^{(0)}(0)|0\rangle + \cdots , \tag{3}$$

and

$$-i\alpha_1(s,\vec{\kappa}^2) = \mu_1(s)\langle\vec{\kappa}|j_4^{(3)}(0)|0\rangle\langle -\vec{\kappa}|j_4^{(3)}(0)|0\rangle . \tag{4}$$

In the infinite-momentum frame the matrix element of a unitary current $j_4^{(\beta)}(0)$, between proton states, can be written as

$$\lim_{p_3, p_3' \to \infty}\langle p'|j_4^{(\beta)}(0)|p\rangle = \left(\frac{m^2}{p_0 p_0'}\right)^{1/2}\bar{u}(p')\left[F_1^\beta(\kappa^2)\gamma_4 + F_2^\beta(\kappa^2)\frac{\sigma_{i4}}{2m}\kappa_i\right]u(p) \quad \text{for } \beta = 0,\ 3, \text{ and } 8. \tag{5}$$

The isovector form factors which enter into the calculation of $\alpha_1(s, \kappa^2)$ are well known. However, the singlet form factors of $\alpha_0(s, \kappa^2)$ are not determined experimentally and we follow Ref. 5 in postulating that they are the familiar isoscalar form factors. In each case the convenient dipole formulas are used to approximate the form factors.[5]

The interaction strength $\mu_0(s)$ is assumed to have a logarithmic energy dependence of the form

$$\mu_0(s) = \mu + \mu'[\ln(s/s_0')]^2, \tag{6}$$

and we again follow Ref. 5 in assuming that $\mu_1(s)$ takes the form

$$\mu_1(s) = \mu\frac{s_0}{s}\exp(i\phi). \tag{7}$$

We find, therefore, that the energy dependence of the model is specified by the interaction constants μ and μ', the scale factors s_0 and s_0', and the phase angle ϕ, which is assumed to have a simple linear dependence on the square of the four-momentum transfer, $-t = \kappa^2$. The total cross section, differential cross sections, and slope parameter $b(s, t)$ are given by

$$\sigma_{\text{tot}}(s) = 4\pi\,\text{Im}\alpha(s, 0),$$
$$\frac{d\sigma}{dt}(s,t) = \pi|\alpha(s,t)|^2, \tag{8}$$
$$b(s,t) \equiv \frac{d}{dt}\left[\ln\frac{d\sigma}{dt}(s,t)\right],$$

and a simple optimization procedure is used to obtain the best over-all agreement with the data. The parameters specifying $\mu_1(s)$, obtained in a previous paper[7] in which the validity of Eq. (7) is assumed, are

$$\mu = 9.76\ \text{GeV}^{-2},$$
$$s_0 = 9\ \text{GeV}^2,$$

and

$$\phi(t = 0) = 85.7°.$$

The values of the remaining parameters determining $\mu_0(s)$ are essentially fixed by the total cross section measurements [see Fig. 1 (Ref. 8)] and are found to be $\mu' = 0.25\ \text{GeV}^{-2}$ and $s_0' = 200\ \text{GeV}^2$.

The slope parameter behaves as shown in Fig. 2 (Ref. 9) in response to two influences. At low energy ($<10^2$ GeV) it increases because the less steeply sloped $I = 1$ exchange term is decreasing with energy, and the steeper slope of the vacuum exchange term is revealing itself. As a result we find the slope parameter b increasing, in this region, like the inverse of the energy dependence of the $I = 1$ exchange. At high energy ($>10^3$ GeV) the slope parameter again increases, in logarithmic fashion now, due to the logarithmic dependence of the vacuum exchange term. A remarkable feature of Fig. 2 is the observed crossover of the slope-parameter curves corresponding to different $-t$ values. This can be seen to be a result of the observed motion in the position of the dips in the differential cross section (see Fig. 3), which move with increasing energy to smaller values of $-t$ (this will be discussed in greater detail later). At a particular value of $-t$, the corresponding slope parameter will be observed to rise with increasing energy as the dip position approaches. Those slope

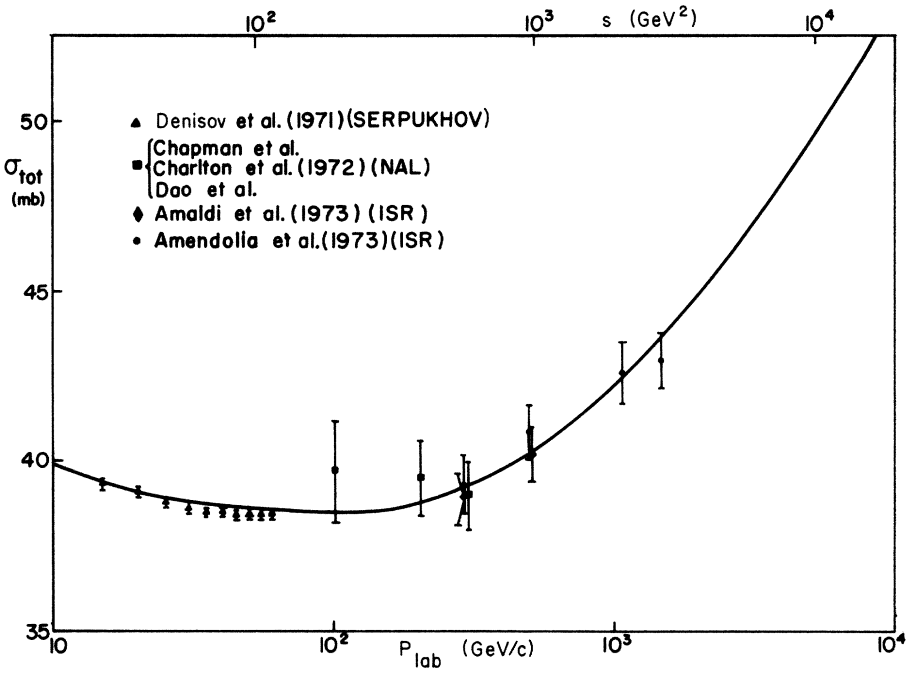

FIG. 1. Total cross section of pp scattering as a function of incident proton laboratory momentum. Data from Refs. 2, 8.

parameters corresponding to higher values of $-t$ will respond first to the approaching dip and, in increasing with energy, will exceed (cross over) those curves corresponding to lower values of $-t$. In the ISR region the slope parameter b would appear to be on a relative plateau region, as is obvious from Fig. 2.

Figure 4 consists of two curves. Of these one (solid line) includes both contributing amplitudes as given by Eqs. (3) and (4), and fits the data very

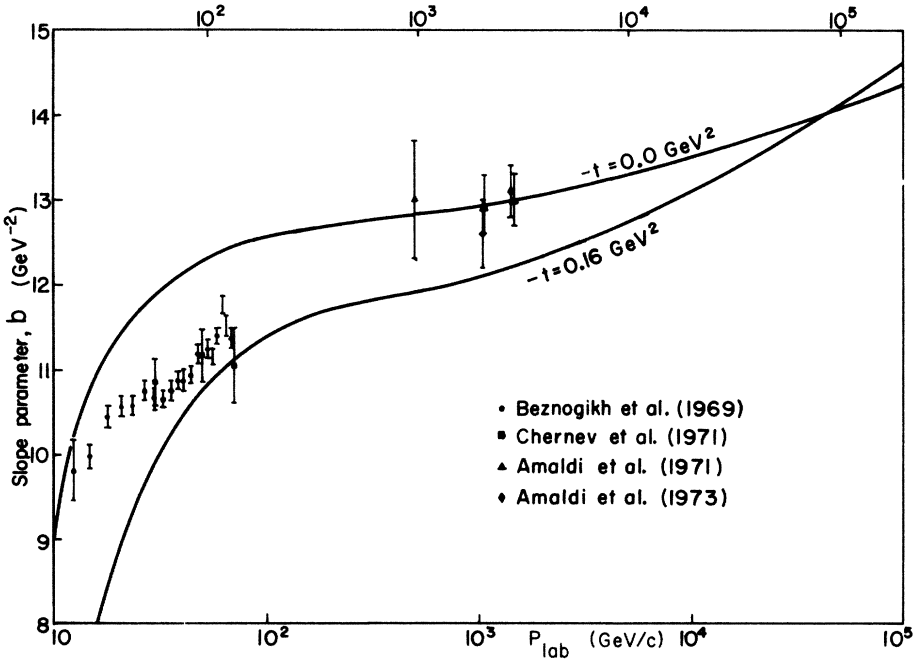

FIG. 2. Slope parameter b of elastic pp scattering as a function of incident-proton laboratory momentum. Data from Ref. 9. The two curves are theoretical values for $t = 0.0$ and $t = -0.16$ GeV^2.

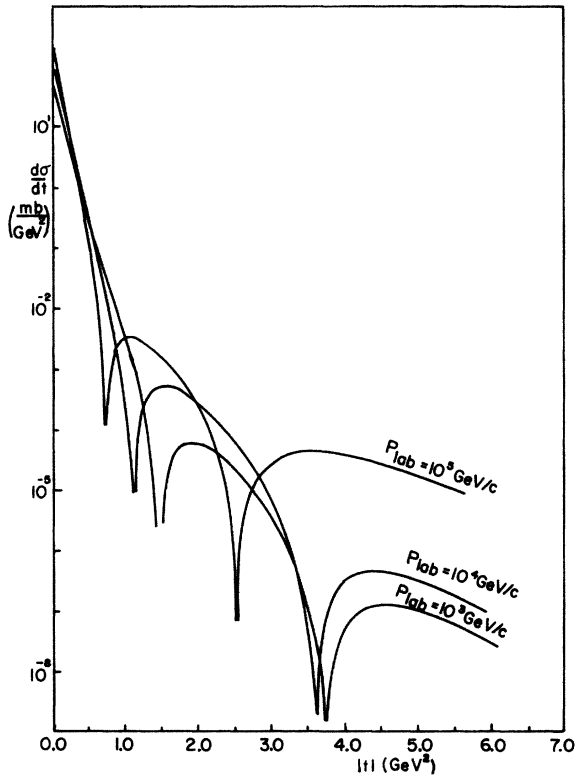

FIG. 3. Theoretical curves for the proton-proton elastic differential cross sections at incident-proton laboratory momenta of 10^3, 10^4, and 10^5 GeV/c. The $I=1$ exchange amplitude has been omitted in order to emphasize the variations in structure with increasing energy due to the vacuum exchange term.

well from $-t=0.0$ to $-t=4.0$. To see the effect of the $I=1$ exchange term we keep only the vacuum exchange term [with $\mu_1(s)=0$], and this is shown as a broken line. It is quite clear that the main features are due to the vacuum exchange term, both of the peaks and the dips. The immediate effect of the $I=1$ exchange term is to mask the dip at $t\cong-1.4$ partially and the dip at $t\cong-3.8$ completely. However, inclusion of the $I=1$ term, which plays a more dominant role at low energy, can fit all data from $P_L=3$ GeV/c upwards. It is not at all important to account for the main feature of pp cross sections above -10^3 GeV/c.

III. DISCUSSION OF THE BEHAVIOR OF THE pp ELASTIC CROSS SECTION AT ENERGIES FROM 10^2 TO 10^5 GeV

At low energy the cross section is decreasing at large $|t|$ at an extremely rapid rate. It is apparent from Fig. 3, however, that the cross section in the large-$|t|$ region is increasing from $P_{lab}=10^3$ GeV/c. This implies the existence of a minimum, say of the secondary peak, between $P_{lab}=10^2$ GeV/c and $P_{lab}=10^3$ GeV/c. The precise height of the secondary peak depends sensitively on the $I=1$ exchange term. Our estimate is that the minimum value of this secondary peak occurs at $P_{lab}\cong 500$ GeV/c. It would be a most striking confirmation of this model if the experiment at NAL should find such a minimum. It is worth remarking, perhaps, that in inclusive spectra at large transverse momentum one finds that the differential cross section is indeed rising from $P_{lab}=100$ GeV/c to $P_{lab}=1000$ GeV/c.[10]

The increase in the height of the peaks as a function of energy is illustrated clearly in Fig. 5. Consider the form of the vacuum exchange amplitude as given by Eq. (3). α_0 consists of a series of alternate positive and negative terms, each of which dominates over a certain t range, leading to a corresponding peak. The significance of the energy-dependent interaction strength $\mu_0(s)$ is that with increasing energy the first peak rises like $(\ln s)^2$, the second peak like $(\ln s)^4$, and the nth peak like $(\ln s)^{2n}$. This is clearly indicated in Fig. 5.

The other immediately obvious feature of Fig. 3 is the motion of the position of the dips in the

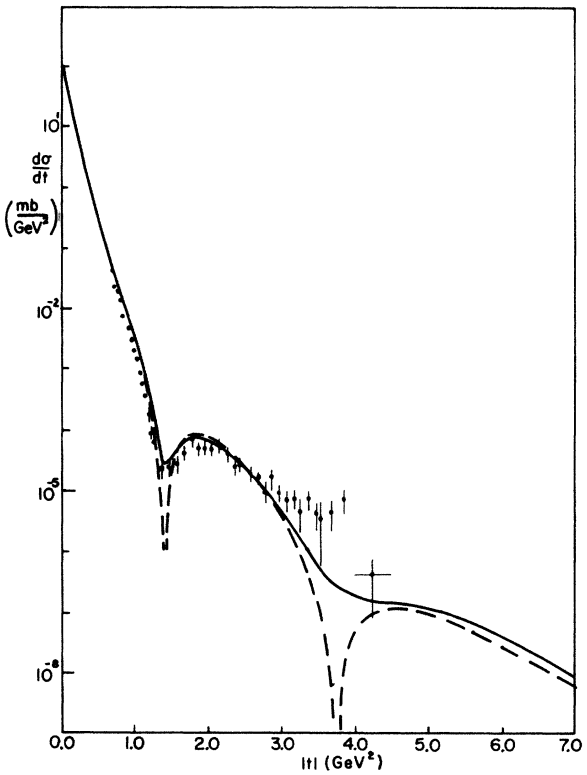

FIG. 4. The theoretical curve for the proton-proton elastic differential cross section at an incident-proton laboratory momentum of 1480 GeV/c. Data from Ref. 1. The broken line corresponds to $\mu_1=0$.

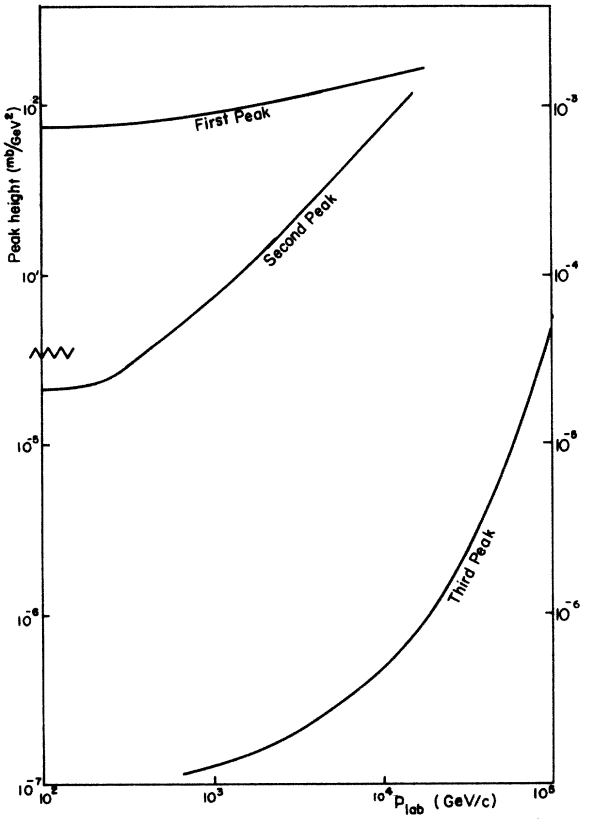

FIG. 5. Theoretical curves for the heights of the first three peaks of the pp elastic differential cross section as functions of incident-proton laboratory momentum.

direction of lower $-t$, or alternatively the narrowing of the peaks, as mentioned earlier. To illustrate clearly the energy dependence of the shifting of the peaks and dips, we plot, in Fig. 6, their positions as a function of energy. The positions of the first dip and the second peak move inward like ln$s$ in the region $P_{lab} = 10^2$–10^5, whereas the positions of the second dip and third peak seem to move faster than ln$s$ as energy increases.

Ultimately, as $s \to \infty$, $\mu_0 \to \infty$. We have the transmission coefficient $s(b) \to 0$; therefore the differential cross section looks like

$$\frac{d\sigma}{dt} \propto \delta(t). \tag{10}$$

IV. COMPARISON WITH THE MODEL OF CHENG AND WU

It is immediately apparent that our model shares some features in common with that of Cheng and Wu, notably in the high-energy limit, where, as $\mu_0 \to \infty$, both models predict a purely absorptive black disk. Direct comparison of the models is readily possible through three distinct features of the Cheng-Wu model:

$$\text{(i)}\ \frac{\sigma_{el}}{\sigma_{tot}} = \tfrac{1}{2} + O((\ln|\delta|)^{-1}), \tag{11}$$

where

$$\delta = \left\{ -\frac{(-s)^a}{[\ln(-s)]^2} + \frac{(-u)^a}{[\ln(-u)]^2} \right\}^{1/a}; \tag{12}$$

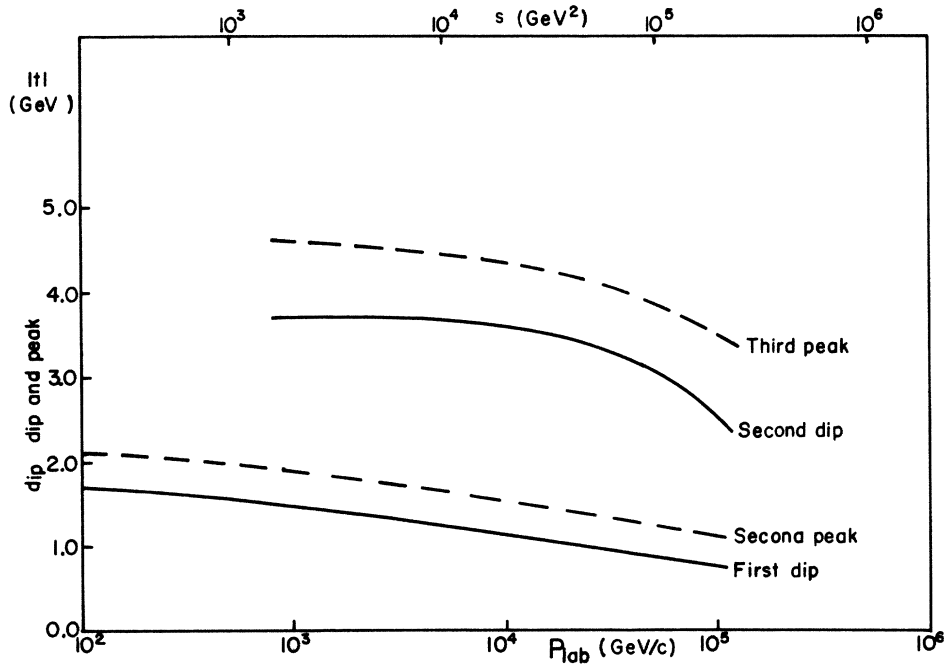

FIG. 6. Theoretical curves for the positions of the dips (solid lines) and the peaks (broken lines) of the pp elastic differential cross section as functions of incident-proton laboratory momentum.

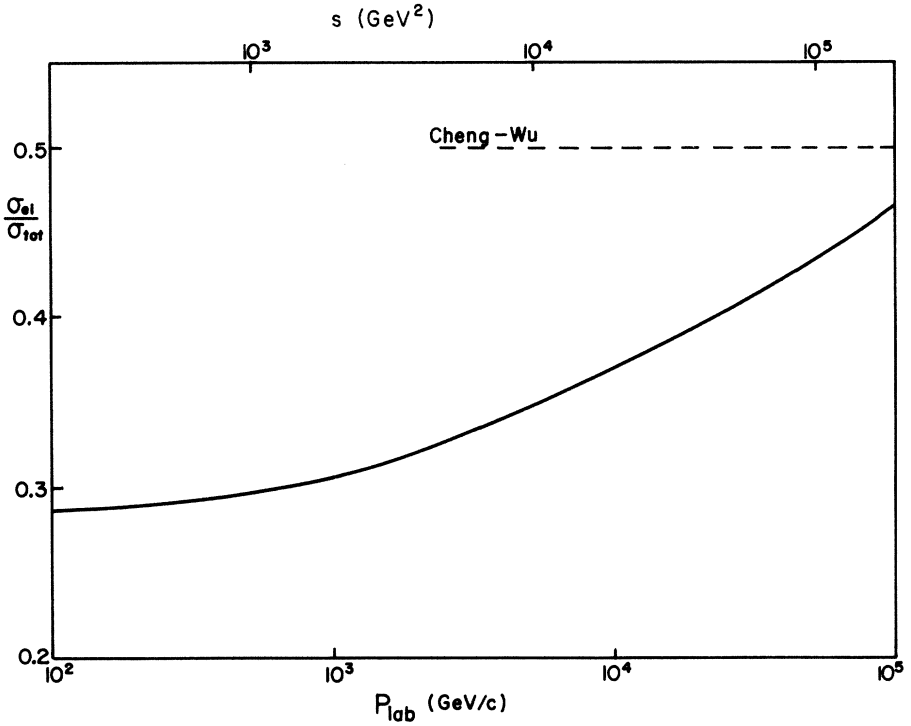

FIG. 7. Theoretical curve for the ratio σ_{el}/σ_{tot} (solid line) as a function of energy. The broken line represents the Cheng-Wu infinite-energy limit $\sigma_{el}/q_{tot} = \frac{1}{2} + O((\ln|s|)^{-1})$.

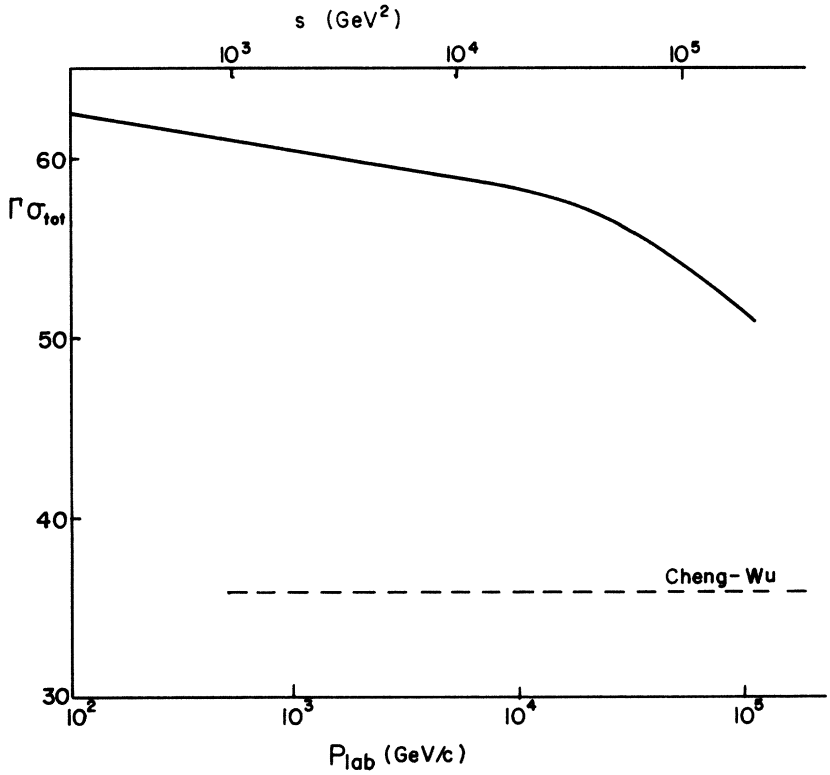

FIG. 8. Theoretical curve for $\Gamma\sigma_{tot}$ as a function of energy, where Γ is the value of $-t$ at which the first dip in the differential cross section occurs. The broken line represents the Cheng-Wu limit, $\Gamma\sigma_{tot} = 35.92 + O((\ln|s|)^{-1})$.

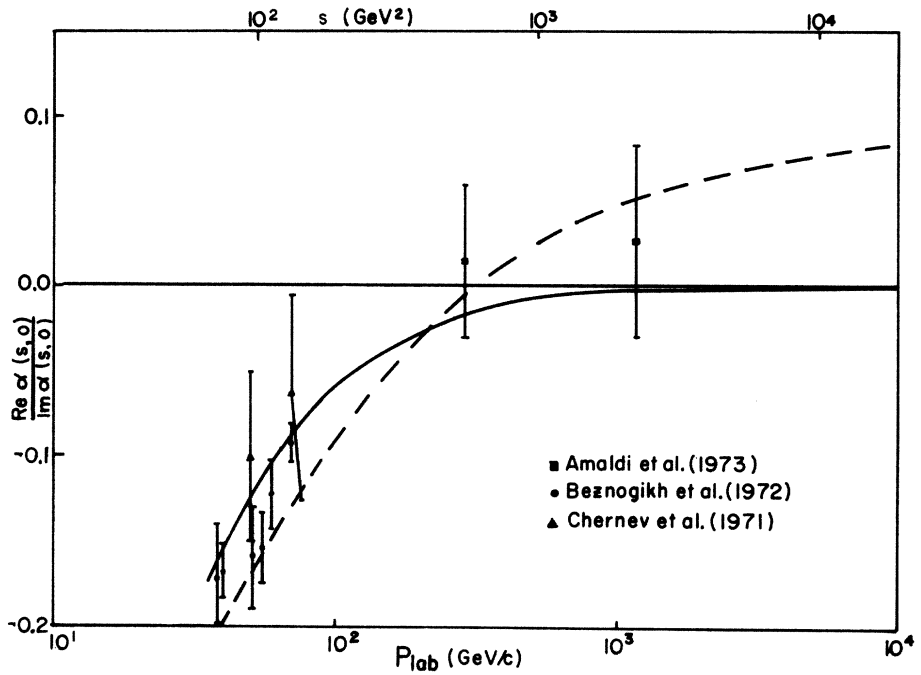

FIG. 9. Theoretical curve for $\mathrm{Re}\alpha(s,0)/\mathrm{Im}\alpha(s,0)$ as a function of energy. The broken line is Cheng and Wu's theoretical curve for the same parameter (Ref. 11). Data from Refs. 9, 12.

$$\text{(ii)}\quad \Gamma\sigma_{\text{tot}} = 35.92 + O((\ln|s|)^{-1}), \tag{13}$$

where Γ is the value of $-t$ at which the first dip occurs;

$$\text{(iii)}\quad \frac{\mathrm{Re}\alpha(s,0)}{\mathrm{Im}\alpha(s,0)} = \frac{\pi}{\ln|s|} + O((\ln|s|)^{-2}). \tag{14}$$

Figures 7–9 provide this direct comparison, plotting the theoretical curves due to our model over the energy range 10^2 GeV to 10^5 GeV and the corresponding curves or high-energy limits given by the Cheng-Wu model. While our curves provide no direct limits, each curve does illustrate fundamental differences between the models. While our theoretical curve in Fig. 7 can be considered consistent with a limiting value of $\sigma_{\text{el}}/\sigma_{\text{tot}} = \frac{1}{2}$, Cheng and Wu approach this limit from above while Fig. 7 would indicate that we approach it from below. In our model $\Gamma\sigma_{\text{tot}}$ is still an energy-dependent quantity and it is not clear from Fig. 8 whether it will approach a constant, much less the predicted value of 35.92. Comparison of the theoretical predictions of both models with experimental data for $\mathrm{Re}\alpha(s,0)/\mathrm{Im}\alpha(s,0)$ and with each other in Fig. 9 (Refs. 9 and 12) illustrates a further significant and possibly experimentally discernible difference. Once again both models have the same infinite-energy limit; however, in our model this limit is effectively attained in an energy region in which the model of Cheng and Wu predicts a value significantly different from zero. In our model the logarithmic increase in amplitude comes from the behavior of μ_0. Hence it only affects the imaginary amplitudes. The real amplitude comes only from the $I=1$ exchange term, and hence when the logarithmic term makes itself felt at $P_{\text{lab}} \sim 10^3$ GeV the ratio of real and imaginary parts must be negligible. Sufficiently accurate data at ISR energies could resolve this question in favor of one or the other of the models. Again the models differ in the manner in which they approach the limit, Cheng and Wu's from above and ours from below.

V. CONCLUDING REMARKS

There is an intrinsic ambiguity in the Chou-Yang model concerning the type of form factors one should choose to use in pp elastic scattering. Our particular version above utilizes the isoscalar form factors. However, it is clear that all the main features discussed above are common to various different choices.[13] Let us summarize our main findings as follows:

(1) At higher energies the slope parameters for two values of t should have a crossover.

(2) The positions of dips and peaks should move inward to smaller $|t|$ values.

(3) The height of the second peak increases faster than that of the first peak, and that of the third increases faster than that of the second, etc.

(4) In the region of the secondary peak, there should exist a minimum around $P_{lab} \cong 500$ GeV/c.

(5) The ratio of real to imaginary parts of the forward amplitudes should be negligible at the present ISR energy.

Especially on the last two points, experiments in progress or to be performed in the near future should be able to prove or disprove them.

---

[1]C. Rubbia, in *Proceedings of the XVI International Conference on High Energy Physics, Chicago-Batavia, Ill., 1972*, edited by J. D. Jackson and A. Roberts (NAL, Batavia, Ill., 1973), Vol. 4, p. 157.

[2]U. Amaldi *et al.*, Phys. Lett. 43B, 231 (1973); S. R. Amendolia *et al.*, *ibid.* 44B, 112 (1973).

[3]We are taking a phenomenological approach here. The fundamental interaction strength remains a constant. The logarithmic dependence may come in when an additional infinite number of Feynman diagrams are accounted for.

[4]T. T. Chou and C. N. Yang, in *High Energy Physics and Nuclear Structure*, edited by G. Alexander (North-Holland, Amsterdam, 1967), p. 348; Phys. Rev. 170, 1591 (1968); Phys. Rev. Lett. 20, 1213 (1968).

[5]S. Y. Lo, Nucl. Phys. B19, 286 (1970).

[6]H. Cheng and T. T. Wu, Phys. Rev. Lett. 24, 1456 (1970).

[7]S. Y. Lo and G. D. Thomson, Nuovo Cimento Lett. 3, 223 (1972).

[8]S. P. Denisov *et al.*, Phys. Lett. 36B, 415 (1971); J. W. Chapman *et al.*, Phys. Rev. Lett. 29, 1686 (1972); G. Charlton *et al.*, *ibid.* 29, 515 (1972); F. T. Dao *et al.*, *ibid.* 29, 1627 (1972).

[9]G. G. Beznogikh *et al.*, Phys. Lett. 30B, 274 (1969); Kh. M. Chernev *et al.*, *ibid.* 36B, 266 (1971); U. Amaldi *et al.*, *ibid.* 36B, 504 (1971); U. Amaldi *et al.*, *ibid.* 44B, 112 (1973).

[10]J. W. Cronin *et al.*, Phys. Rev. Lett. 31, 1426 (1973); B. Alper *et al.*, Phys. Lett. 44B, 521 (1973).

[11]H. Cheng, J. K. Walker, and T. T. Wu, Phys. Lett. 44B, 283 (1973).

[12]G. G. Beznogikh *et al.*, Phys. Lett. 39B, 411 (1972).

[13]M. Kac, Nucl. Phys. B62, 402 (1973).